

### VASCULAR BIOLOGY

# Impaired adhesion of neutrophils expressing Slc44a2/HNA-3b to VWF protects against NETosis under venous shear rates

Gaïa Zirka,<sup>1</sup> Philippe Robert,<sup>2,3</sup> Julia Tilburg,<sup>4</sup> Victoria Tishkova,<sup>5</sup> Chrissta X. Maracle,<sup>4</sup> Paulette Legendre,<sup>6</sup> Bart J. M. van Vlijmen,<sup>4</sup> Marie-Christine Alessi,<sup>1,7</sup> Peter J. Lenting,<sup>6</sup> Pierre-Emmanuel Morange,<sup>1,7</sup> and Grace M. Thomas<sup>1</sup>

<sup>1</sup>Aix-Marseille University, INSERM, Institut National de Recherche pour l'Agriculture, l'Alimentation et l'Environnement (INRAE), Center for CardioVascular and Nutrition Research (C2VN), Marseille, France; <sup>2</sup>Aix-Marseille University, Centre National de la Recherche Scientifique (CNRS), INSERM, Adhesion and Inflammation Laboratory, Marseille, France; <sup>3</sup>Laboratoire d'Immunologie, Assistance Publique-Hôpitaux de Marseille (AP-HM), Centre Hospitalier Universitaire de la Conception, Marseille, France; <sup>4</sup>Eindhoven Laboratory for Experimental Vascular Medicine, Division of Thrombosis and Hemostasis, Department of Internal Medicine, Leiden University Medical Center, Leiden, The Netherlands; <sup>5</sup>Aix-Marseille University, CNRS, Centre Interdisciplinaire de Nanoscience de Marseille (CINaM), Marseille, France; <sup>6</sup>INSERM, Unité Mixte de Recherche en Santé (UMR-S) 1176, Université Paris-Sud, Université Paris-Saclay, Le Kremlin-Bicêtre, France; and <sup>7</sup>Laboratoire d'Hématologie, AP-HM, Centre Hospitalier Universitaire de la Timone, Marseille, France

**KEY POINTS**

- **Slc44a2 expressed by neutrophils is important for their adhesion to VWF-A1 domain and can mediate NETosis on VWF at venous shear.**
- **Slc44a2 importance in neutrophil recruitment on VWF is exacerbated during inflammation both in vitro and in vivo.**

**Genome-wide association studies linked expression of the human neutrophil antigen 3b (HNA-3b) epitope on the Slc44a2 protein with a 30% decreased risk of venous thrombosis (VT) in humans. Slc44a2 is a ubiquitous transmembrane protein identified as a receptor for von Willebrand factor (VWF). To explain the link between Slc44a2 and VT, we wanted to determine how Slc44a2 expressing either HNA-3a or HNA-3b on neutrophils could modulate their adhesion and activation on VWF under flow. Transfected HEK293T cells or neutrophils homozygous for the HNA-3a- or HNA-3b-coding allele were purified from healthy donors and perfused in flow chambers coated with VWF at venous shear rates (100 s<sup>-1</sup>). HNA-3a expression was required for Slc44a2-mediated neutrophil adhesion to VWF at 100 s<sup>-1</sup>. This adhesion could occur independently of β<sub>2</sub> integrin and was enhanced when neutrophils were preactivated with lipopolysaccharide. Moreover, specific shear conditions with high neutrophil concentration could act as a "second hit," inducing the formation of neutrophil extracellular traps. Neutrophil mobilization was also measured by intravital microscopy in venules from SLC44A2-knockout and wild-type mice after histamine-induced endothelial**

**degranulation. Mice lacking Slc44a2 showed a massive reduction in neutrophil recruitment in inflamed mesenteric venules. Our results show that Slc44a2/HNA-3a is important for the adhesion and activation of neutrophils in veins under inflammation and when submitted to specific shears. The fact that neutrophils expressing Slc44a2/HNA-3b have a different response on VWF in the conditions tested could thus explain the association between HNA-3b and a reduced risk for VT in humans. (Blood. 2021;137(16):2256-2266)**

## Introduction

Venous thromboembolic disease is the third leading cause of cardiovascular death after myocardial infarction and stroke in industrialized countries. Venous thrombosis (VT) is a multifactorial disease whose mechanisms still remain to be fully uncovered. Until recently, pathophysiology of VT was only based on the original cascade model of coagulation. Accumulating data have highlighted mechanisms independent of the coagulation cascade on clot formation.

Using genome-wide association study approaches and transgenic mice, our team and others have contributed to the identification of SLC44A2 as a new gene involved with VT both in humans<sup>1,2</sup> and in mice.<sup>3-5</sup> In-depth analysis of the SLC44A2 locus identified

rs2288904 (461G>A; Arg154Gln) as the functional variant responsible for the association with VT. This polymorphism defines the expression of the human neutrophil antigen 3a (HNA-3a; 461G; Arg154) or HNA-3b (461A; Gln154) by the choline transporter-like protein 2 (also called Slc44a2 protein) encoded by the SLC44A2 gene.<sup>6-8</sup> Homozygosity for the HNA-3b-coding allele is associated with a decreased risk of VT (~30%).<sup>1</sup>

Slc44a2 is an ubiquitous transmembrane protein of 70 to 95 kDa<sup>9</sup> that was identified as a new receptor for von Willebrand factor (VWF) in 2015<sup>10</sup> and a receptor for VWF-primed platelets through α<sub>IIb</sub>β<sub>3</sub> interaction in 2020.<sup>11</sup> Slc44a2 has been associated with transfusion acute-lung injury (TRALI), which is one of the leading causes of transfusion-associated mortality in developed countries.<sup>12</sup>

Severe cases have been associated with alloantibodies reacting against the Slc44a2/HNA-3a epitope, the same antigen associated with VT. We and others have shown that alloantibodies targeting Slc44a2 can lead to neutrophil activation and formation of neutrophil extracellular traps (NETs) by primed HNA-3a<sup>+</sup> neutrophils.<sup>13,14</sup> Platelet and neutrophil recruitment to the endothelium and cell activation/NETosis are key steps not only in TRALI<sup>14,15</sup> but also in arterial thrombosis<sup>16</sup> and VT.<sup>17-19</sup> After adhesion to the activated endothelium, neutrophils initiate and propagate VT by interacting with platelets and exposure of tissue factor and active FXII.<sup>18</sup> Importantly, mice with impaired NETosis have a decreased incidence of thrombosis in a model of VT,<sup>20</sup> and mice treated with DNase-1 (which degrades DNA and NETs) are protected in this model.<sup>17</sup> As for thrombosis, outcome of mice with TRALI could be improved by DNase-1 inhalation<sup>14</sup> The TRALI model, may pave the way to understand why Slc44a2 plays a role in VT and why HNA-3b isoform carriers have a decreased risk of VT. We investigated in this study whether Slc44a2 could act as an adhesion protein allowing neutrophil adhesion to VWF under flow and whether Slc44a2 could act as a receptor able to activate neutrophils and stimulate NETosis.

We demonstrated that Slc44a2 is important in the adhesion and activation process of neutrophils under flow when submitted to inflammation and specific shear conditions. The fact that neutrophils expressing Slc44a2/HNA-3b show reduced rolling and activation on VWF could thus explain the association between the HNA-3b epitope and the reduced risk of VT in humans.

## Methods

### Cell lines and culture

HEK293T cells stably transfected to express Slc44a2/HNA-3a (R154) or Slc44a2/HNA-3b (Q154) fused with a GFP tag were generous gifts from Daniel Bougie and Brian Curtis (Blood Center of Wisconsin, Milwaukee, WI). Cells were cultured as previously described.<sup>8,21</sup> Phosphate-buffered saline (PBS) and Versene (0.48 mM; Gibco) were used for cell dissociation.

### Human neutrophil isolation

After all participants gave written informed consent, neutrophils were isolated at Timone University Hospital (Marseille, France) from the blood of healthy volunteers who declared that they had not received any medication for at least 2 weeks. Sodium citrate was used as anticoagulant for blood puncture, except if otherwise specified. Neutrophils were prepared as previously described.<sup>14</sup> The research was approved by the relevant institutional review boards and ethics committees. The investigation conforms to the principles outlined in the Declaration of Helsinki. After isolation, neutrophils were eventually labeled with the fluorescent dye of use. When specified, 1 mM CaCl<sub>2</sub> and/or blocking antibodies were added to neutrophils before utilization. Concentration was adjusted, and only cells at acceptable viability (>75%) were used.

### SLC44A2 genotyping

Donors homozygous for the HNA-3a- or HNA-3b-coding allele were identified by single-nucleotide polymorphism genotyping using a TaqMan 5' exonuclease polymerase chain reaction technology as previously described.<sup>22</sup>

### Flow chamber assays

Flow chamber  $\mu$ -slide VI 0.1 ibitreat (Ibidi) was used for cell velocity analysis and NETosis experiments. Vena8 Fluoro + Microfluidic Biochip (Cellix) was used for NETosis experiments. Chambers were coated overnight at 4°C with 70  $\mu$ g/mL VWF (Wilfactin, LFB), VWF recombinant A1-Fc domain (10  $\mu$ g/mL), fibrinogen (10  $\mu$ g/mL), or bovine serum albumin (BSA; 10  $\mu$ g/mL; Sigma-Aldrich). Saturation was done with PBS/BSA 0.1% 1 hour prior to the assay. If applicable, blocking antibodies (10  $\mu$ g/mL; VWF-A1 blocking Ab 318 clone, anti-CD18 TS1/18 clone, irrelevant immunoglobulin G1 [IgG1] or IgG2) were incubated in the channels and with neutrophils 30 minutes before cell perfusion and perfused concomitantly at 25  $\mu$ g/mL for VWF blockade experiments. Continuous flow rate was applied forward using an electrical syringe pump (Bioblock Scientific), a Terumo syringe, and silicon tubing. One channel was used per condition, and the chambers were discarded after each experiment.

HEK293T cells or purified neutrophils were labeled for 20 minutes under gentle agitation with Calcein AM (4  $\mu$ M; Invitrogen), Cell trace red orange (4  $\mu$ M; Invitrogen), or DiD dye (2  $\mu$ g/mL) for experiments including cell activation. Cells were washed from the dye excess after staining. When indicated, neutrophils were incubated with lipopolysaccharide (LPS; 5 or 25  $\mu$ g/mL) or MnCl<sub>2</sub> (1 mM) for 1 hour prior to cell perfusion and eventually incubated 5 minutes before the experiment with calcium (1 mM). Extracellular DNA was labeled by addition of Sytox Green or Sytox Red (1  $\mu$ M; Invitrogen) to the neutrophils immediately before perfusion. A total of  $1.5 \times 10^6$  cells per mL (or other if specified) were infused in flow chamber at a wall shear rate of 100 s<sup>-1</sup> (or other if specified) at a controlled temperature of 37°C using a thermoregulated thermostatic chamber (Olympus). Cells were allowed to pass through the channel for 5 minutes before acquisition. For immunostaining experiments, neutrophils accumulated at the entrance of the chamber after perfusion at 100 s<sup>-1</sup> were fixed using zinc fixative. Nonspecific binding sites were blocked with Tween/BSA, and cells were stained overnight at 4° for myeloperoxidase (MPO; mouse monoclonal IgG anti-human MPO, 2  $\mu$ g/mL; Abcam) and citrullinated histone H3 (rabbit polyclonal anti-human H3cit, 2  $\mu$ g/mL; Abcam). Goat anti-rabbit IgG-Alexa Fluor 488 and goat-anti-mouse IgG-Alexa Fluor 647 (4  $\mu$ g/mL; Invitrogen) were used as secondary antibodies. Irrelevant antibodies were used for negative control (2  $\mu$ g/mL; mouse IgG from BioLegend and rabbit IgG from Abcam). Hoechst 33342 (1  $\mu$ g/mL) was used for DNA staining. Acquisition was done with an inverted microscope (IX71; Olympus) and a LED fluorescence lamp for sample excitation (SPECTRA X light engine, Lumencor) in 3 different fields (1329.4  $\mu$ m wide) during 1 minute at a rate of 50 images per second. Real-time imaging was performed using a CMOS digital camera (Orca-Flash 4.0 V2 CCD C11440; Hamamatsu).

### Flow chamber cell motion analysis

A dedicated program was written in Java (Oracle) as a plugin for ImageJ (National Institutes of Health). More details are given in supplemental Methods (available on the *Blood* Web site).

### NET generation in vitro

NET generation was done and quantified as previously described.<sup>14</sup> Tumor necrosis factor- $\alpha$  (TNF $\alpha$ ) was used for cell priming, because TNF- $\alpha$  is produced by human neutrophils stimulated by LPS<sup>23</sup> and has been commonly used for this assay in other studies.

## Model of endothelial degranulation on mouse mesenteric venules

Twelve-week-old *SLC44A2* knockout (KO) male mice (C57BL/6J background) and wild-type littermate controls were used to investigate neutrophil recruitment upon endothelial degranulation as previously done.<sup>20</sup> Experimental animal procedures were approved by local welfare committees in Aix-Marseille University. Experiments were performed blinded for genotype. More details are given in supplemental Methods.

**Numerical simulations** Numerical simulations were realized in finite elements (Comsol Multiphysics) in 2 steps. First, a stationary study of the fluid flow is performed in order to solve the Navier-Stokes equation. The following parameters were used: fluid was considered as water, with water density and viscosity at 37°C, as protein and ion-induced changes are nonsignificant at physiological concentrations. Fluid velocity at wall contact was 0. Flow was identical at what was experimentally set for cell experiments (4  $\mu\text{L}/\text{min}$  for Cellix chambers, 10  $\mu\text{L}/\text{min}$  for Ibidi chambers). Dimensions of the chambers were given by the respective manufacturers. Second, trajectories for each cell in the fluid were calculated, and gravity was taken into account. A time-dependent study was performed for 60 seconds. Cells were represented by spheres of radius 10  $\mu\text{m}$  and density 1.08, corresponding to the average human polymorphonuclear size and density. Each contact of a cell with the considered wall was counted as 1.

## Statistical analysis

A Shapiro-Wilk test was used to check normality. Immunofluorescence data were analyzed with a 1-way analysis of variance test, rolling data with a nested t test, and NETosis quantification and in vivo data with an unpaired t test. Results were considered significant if  $P < .05$ .

## Results

### The *Slc44a2*/HNA-3a epitope is necessary for cell adhesion to VWF under flow

We used HEK293T cells expressing either *Slc44a2*/HNA-3a (Arg154) or *Slc44a2*/HNA-3b (Gln154). These cells have been already characterized and have been shown to express similar levels of *Slc44a2*<sup>8</sup> (verified by western blot by detecting *Slc44a2*-coexpressed GFP, supplemental Figure 1). After coincubation of cells with purified VWF, we observed patches positive for VWF staining that were 2.6-fold more intense on HEK293T/HNA-3a<sup>+</sup> than on HEK293T/HNA-3b<sup>+</sup> cells (Figure 1). We then perfused fluorescently transfected HEK293T cells in flow chambers pre-coated with VWF and submitted to a “postcapillary venule” shear rate of 100  $\text{s}^{-1}$ . Digital real-time imaging of the flowing cells allowed digital analysis of the velocity data. We plotted the frequency distribution of cell velocities from each of the 3 different fields analyzed. We observed a maximum of cells  $\sim 1400$  to 1600  $\mu\text{m}/\text{s}$  (Figure 2A) corresponding to the nonsedimented population for both groups. We also detected some cells interacting strongly with the matrix (speed  $< 10 \mu\text{m}/\text{s}$ ) in the HNA-3a<sup>+</sup> group. We compiled the cell velocities in 2 different populations: “slow rolling” ( $< 10 \mu\text{m}/\text{s}$ ) and “rolling” (200–500  $\mu\text{m}/\text{s}$ ). Exposure of HNA-3a by HEK293T cells allowed cell adhesion/slow rolling to the VWF matrix under flow, whereas HEK293T/HNA-3b<sup>+</sup> cells lost this ability (1.32%  $\pm$  0.60% against 0% of total tracked cells adhering to the matrix, respectively; Figure 2B).

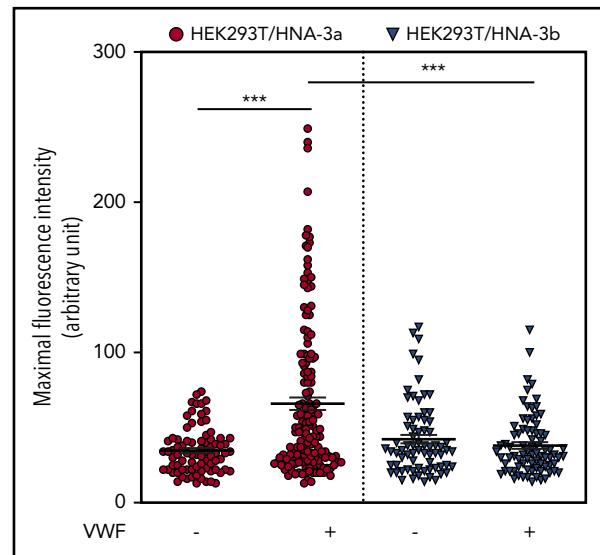


**Figure 1. HEK293T/HNA-3a cells bind more to VWF than HEK293T/HNA-3b cells.** Quantification of maximal fluorescence intensity recorded per cell and representing anti-VWF staining on transfected HNA-3a<sup>-</sup> (red circle) or HNA-3b<sup>-</sup> expressing HEK293T cells (blue triangle). Each dot represents 1 cell with  $n = 81, 153, 72,$  and  $80$  cells analyzed, respectively, for the HNA-3a-VWF, HNA-3a+VWF, HNA-3b-VWF, and HNA-3b+VWF groups (mean  $\pm$  SEM; 1-way analysis of variance test, \*\*\* $P < .005$ ).

We wondered if *Slc44a2* could also modulate neutrophil recruitment to VWF, which is crucial in VT. We repeated the previous experiment by replacing HEK293T cells with purified blood neutrophils from donors homozygous for either the HNA-3a<sup>-</sup> or HNA-3b<sup>-</sup> coding allele. As expected, we found the majority of the neutrophils as nonsedimented with a speed of  $\sim 1500$  to 1600  $\mu\text{m}/\text{s}$ . We also observed cells rolling at a speed of  $\sim 300 \mu\text{m}/\text{s}$  (Figure 2C). Here again, the HNA-3a/3b epitope did not influence the rolling population on VWF, whereas HNA-3b<sup>+</sup> neutrophils showed a significant reduction in the slow-rolling population on this matrix (Figure 2D; supplemental Videos 1 and 2). This was not observed in presence of higher shear rates (1000  $\text{s}^{-1}$ ; data not shown). We could inhibit HNA-3a-dependent adhesion with a specific VWF-A1 domain blocking antibody (Figure 2E). These data suggest that the HNA-3b epitope expressed by *Slc44a2* may reduce cell adhesion to VWF under venous shear rates.

### Neutrophil adhesion on VWF under flow is amplified after an inflammatory first “hit”

Inflammatory-related disorders often follow the 2/multiple-hit hypothesis. HNA-3a-associated VT probably follows this pattern, and this may explain why not all the HNA-3a<sup>+</sup> population will suffer from VT. The difference between the HNA-3a<sup>+</sup> and HNA-3b<sup>+</sup> groups was also present when lower shear rates were applied (50 and 10  $\text{s}^{-1}$ ; Figure 3A), with a significant increase in the slow-rolling population for HNA-3a<sup>+</sup> cells alone. We also tested an inflammatory hit mimicking an infection. We preactivated neutrophils with LPS (5 or 25  $\mu\text{g}/\text{mL}$ ) for 1 hour before perfusion. Since neutrophils lose their capacity to retain Calcein dyes during activation,<sup>24</sup> we stained the cells with a lipophilic membrane dye to permit cell tracking after LPS challenge. Our data show that LPS increases slow rolling of HNA-3a<sup>+</sup> neutrophil on VWF at 100  $\text{s}^{-1}$ , whereas HNA-3b<sup>+</sup> neutrophils seem to not be affected by LPS challenge (Figure 3B). LPS did not affect rolling for the 200 to 500  $\mu\text{m}/\text{s}$  velocity range (Figure 3C). This increase in cell adhesion

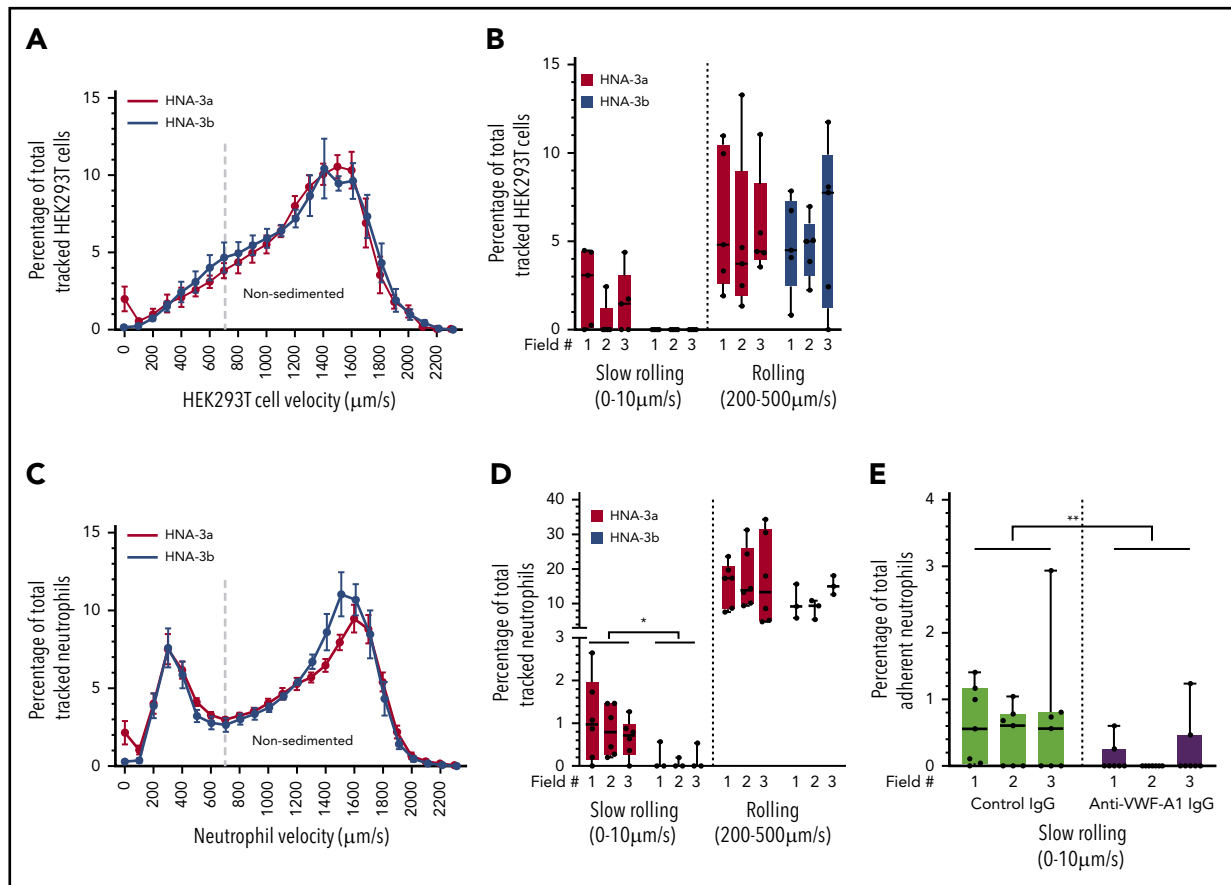


**Figure 2. The Slc44a2/HNA-3a epitope is necessary for cell slow rolling to VWF under flow.** (A,C) Compiled amount of HEK293T cells (n = 5 independent experiments) (A) or neutrophils (HNA-3a, n = 6 donors; HNA-3b, n = 3 donors) (C) counted in function of their mean velocity ( $\mu\text{m/s}$ ) on coated VWF when submitted to a  $100 \text{ s}^{-1}$  shear rate. The dashed line separates sedimented (left) from nonsedimented cells (right). Red, HNA-3a-expressing cells; blue, HNA-3b-expressing cells. (B,D-E) Graphs depicting the slow-rolling and rolling profiles of HEK293T cells (B) and neutrophils (D-E) perfused on a VWF matrix under flow at a  $100 \text{ s}^{-1}$  shear rate. Perfusion of cells at  $100 \text{ s}^{-1}$  resulted in more slow rolling of Slc44a2/HNA-3a-expressing HEK293T cells (B; n = 5 independent experiments) and neutrophils (D; HNA-3a n = 6 donors; HNA-3b n = 3 donors) to human VWF-coated channels compared with Slc44a2/HNA-3b-expressing cells (blue). Slow rolling of Slc44a2/HNA-3a-expressing neutrophils (E, n = 7 donors) to VWF were blocked by VWF-A1 domain-blocking monoclonal antibody (control IgG, light green; anti-VWF-A1-IgG, purple). Data are represented in nested form, and values obtained for each field are shown. Three fields were analyzed for each experiment/donor. (A,C) Mean  $\pm$  SEM; (B-D) nested t test, minimum/maximum, quartiles, and medians are represented. \* $P < .05$ ; \*\* $P < .01$ ; \*\*\* $P < .005$ .

suggested an integrin-dependent process. Because  $\beta_2$  integrins can bind VWF, we assessed their contribution in our model without inflammatory stimulation. We treated HNA-3a/HNA-3b<sup>+</sup> neutrophils with either a specific  $\beta_2$ -blocking antibody or an irrelevant antibody (Figure 3D-E).  $\beta_2$  integrin blockade did not abolish neutrophil slow rolling to VWF at  $100 \text{ s}^{-1}$ , showing that Slc44a2/HNA-3a-mediated neutrophil adhesion to VWF is at least partly  $\beta_2$ -integrin independent. Taken together, these data show that adhesion of HNA-3a<sup>+</sup> neutrophils to VWF is amplified by LPS and does not depend only on  $\beta_2$  integrins, whereas HNA-3b<sup>+</sup> neutrophils do not seem to be affected by LPS in VWF adhesion experiments.

### Slc44a2/HNA-3b neutrophils are protected from NETosis on VWF at venous shear rates

The enhanced neutrophil adhesion observed for the Slc44a2/HNA-3a<sup>+</sup> group after LPS treatment prompted us to evaluate Slc44a2 involvement in neutrophil activation such as NETosis. NETosis is crucial during VT, and it has already been described in TRALI after antibody binding to HNA-3a following a double-hit scheme. We reproduced this pattern, priming neutrophils with LPS and modulating an additional factor that could trigger VT. During stasis, local concentrations in leukocytes can increase.

We perfused different concentrations of LPS-primed neutrophils through a VWF-coated flow chamber. Fluorescence intensity visualization was set up to focus on cell accumulation and not flowing cells. Cells were flowing normally at the  $1.5 \pm 10^6$  cells per mL concentration in Ibidi chambers (Figure 4A, upper left panel). However, increasing the perfused cell concentration induced an accumulation of neutrophils (red, Calcein red orange) sticking together and to the coated surface. The staining of extracellular DNA (yellow, Sytox green) indicates that these neutrophils form NETs, as shown by the presence of DNA fibers escaping from the cells (Figure 4A, upper middle and right panels; supplemental Video 3). This phenomenon was also observed when another chamber brand was used (Cellix) (Figure 4A, lower panels; supplemental Video 4 after 5 minutes of perfusion and supplemental Video 5 after 15 minutes of perfusion). Costaining of the cell accumulation at the entrance of the channel for DNA, H3cit, and MPO confirmed that these fibers had hallmarks of NETs in both brands of chamber slides (Figure 4B). In vitro incubation of TNF $\alpha$ -primed HNA-3a<sup>+</sup> neutrophils with VWF resulted in an increase in the percentage of NET-forming cells (Figure 4C-D). This supports the hypothesis that Slc44a2/HNA-3a can mediate neutrophil activation and NETosis in presence of VWF.

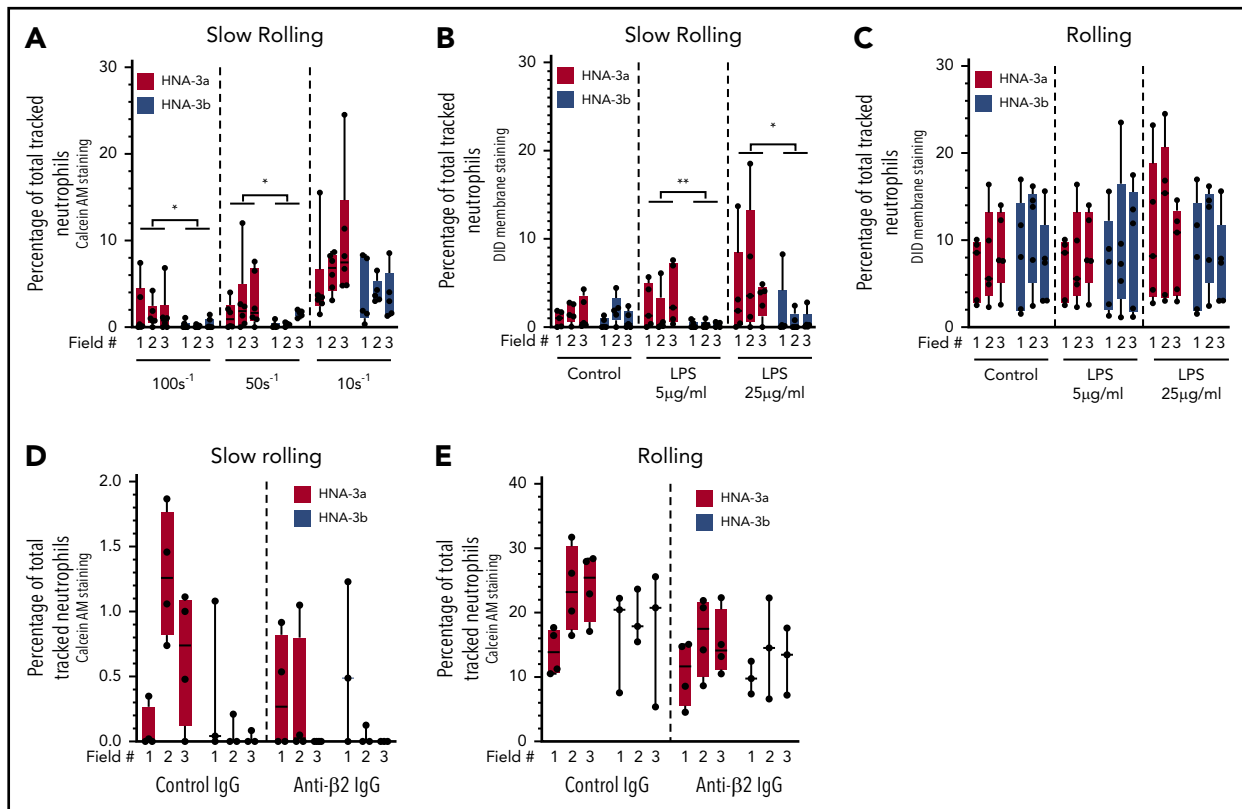


**Figure 3. Adhesion of HNA-3a-expressing neutrophils to VWF is amplified by LPS and does not require  $\beta_2$  integrins.** (A) Percentage of total tracked neutrophils qualified as in slow rolling when perfused at  $100\text{ s}^{-1}$ ,  $50\text{ s}^{-1}$ , and  $10\text{ s}^{-1}$  on immobilized VWF (HNA-3a, red,  $n = 6$  donors per condition; HNA-3b, blue,  $n = 6$  donors for  $100\text{ s}^{-1}$  and 5 donors for  $50\text{ s}^{-1}$  and  $10\text{ s}^{-1}$ ). (B-C) Percentage of total tracked neutrophils qualified as slow rolling (B) or rolling (C) when perfused at  $100\text{ s}^{-1}$  on immobilized VWF after LPS treatment (5 or  $25\text{ }\mu\text{g/ml}$ ) prior to perfusion ( $n = 5$  donors per condition). (D-E) Percentage of total tracked neutrophils qualified as slow rolling (D) or rolling (E) when perfused at  $100\text{ s}^{-1}$  on immobilized VWF after treatment with a  $\beta_2$  integrin blocking IgG or a control irrelevant IgG (HNA-3a, red,  $n = 4$  donors; HNA-3b, blue,  $n = 3$  donors per condition). Data are represented in nested form, values obtained for each field are shown, and 3 fields were analyzed for each experiment/donor (minimum/maximum, quartiles and medians are represented; nested t test; \* $P < .05$ ; \*\* $P < .01$ ).

We performed numerical simulations of the rheological conditions in both chamber brands. We confirmed that the simulated shear rates in contact with the chamber walls of the observation channel are indeed in the desired values (ie,  $100\text{ s}^{-1}$ ) (Figure 5A). However, flow conditions at the chamber entrance (where the vertical inlet cylindrical channel meets the rectangular section observation channel) show much lower shear rate, toward a few  $\text{s}^{-1}$  (Figure 5A-B). When compared with the first half of the well, this area is characterized by liquid and cells regaining speed (Figure 5B). We made digital simulations of cell having made contact with the vertical inlet bottom after 1 minute of cell perfusion. In Cellix chambers, cells are homogeneously deposited at the bottom of the vertical inlet, whereas more cells accumulate there for Ibidi, but mostly at the corner (croissant shape) (Figure 5C). Interestingly, we observed that NETosis occurs in this area of low shear, starting more often in the second half of the vertical inlet bottom (Figure 5D). NETosis occurred at lower cell concentration in the Cellix chamber entrance, for which the speed of liquid is mostly higher than in the Ibidi chamber. This suggests from a rheologic perspective that cell speed, cell concentration, and a minimal shear stress are essential to observe Slc44a2/VWF-mediated NETosis under flow.

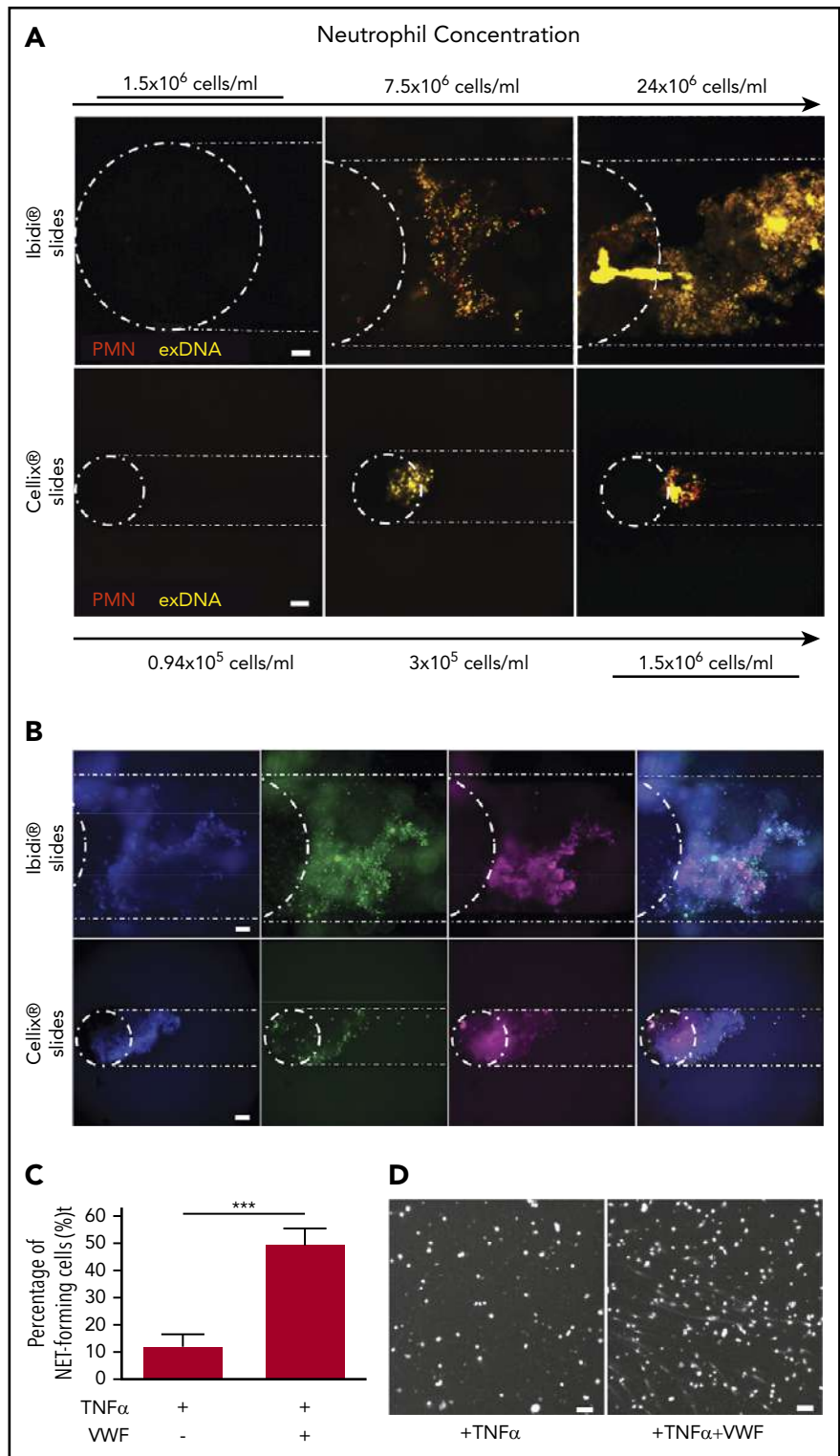
Slc44a2/VWF-mediated NETosis under flow can be amplified by increasing the intensity of the inflammatory stimulus from 5 to  $25\text{ }\mu\text{g/ml}$  LPS for the 2 different brands of flow chambers used (supplemental Figure 3; Figure 6A). However, HNA-3b<sup>+</sup>

neutrophils did not form extracellular DNA structures (Figure 6A, right panels). This HNA-3a-dependent cell accumulation was an all-or-nothing phenomenon (total  $n = 45$  channels tested in 5 independent experiments). It was calcium dependent, showing that extracellular DNA trap formation is an active phenomenon following the adhesion of neutrophils to the immobilized VWF under flow. We tested different matrices, such as BSA, fibrinogen, and VWF-A1 domain, and confirmed to be in the presence of a VWF-A1-dependent phenomenon (Figure 6B). These results show that even under inflammatory stimulation, the HNA-3b epitope is protective against NETosis on VWF at venous shear rates in vitro.

### Slc44a2 plays a major role in neutrophil recruitment at the vessel wall after endothelial degranulation in vivo

In order to confirm our data in vivo, and because mice “knocked in” for our polymorphism of interest are not yet accessible, we used SLC44A2 KO mice and submitted them to the model of histamine-induced endothelial degranulation. Endothelial degranulation results in VWF release from the Weibel-Palade bodies. Mouse infusion with fluorescently labeled anti-Ly-6G antibody allowed us to track neutrophil accumulation at the vessel wall in this model. Our data confirmed our in vitro hypothesis, and we observed a drastic reduction in neutrophil rolling and adhesion at the vessel wall of mesenteric venules in the absence of Slc44a2 (Figure 7;  $409 \pm 300$  cells per minute vs  $59 \pm 26$  cells per minute).

**Figure 4. Primed neutrophils in contact with VWF can form DNA extracellular traps.** (A) Representative images of fluorescently labeled LPS-primed neutrophils (PMN, red) and extracellular DNA (exDNA, yellow) after perfusion ( $100 \text{ s}^{-1}$  shear rate) on VWF of different concentrations of neutrophils in 2 different brands of flow chambers (n = 2 donors per chamber brand). Dashed lines have been added to delimit flow channels and the well entrance. (B) Representative images of fluorescently labeled NETs at the chamber entrance showing total DNA (Hoechst 33342, blue), H3cit (green), and MPO (pink) staining after perfusion of neutrophils in Ibidi slides at  $24 \times 10^6$  cells per mL (upper panel, n = 3 donors and 9 channels) and in Cellix slides at  $1.5 \times 10^6$  cells per mL (lower panel, n = 2 donors and 4 channels) (C-D) Quantification of NETs after VWF challenge by fluorescence microscopy analysis. HNA-3a<sup>+</sup> neutrophils were primed with TNF $\alpha$  (to mimic LPS activation) and incubated for 180 minutes with PBS (+TNF $\alpha$ ) or VWF (+TNF $\alpha$ +VWF). DNA release was visualized after DNA staining with Hoechst 33342 (n = 9 fields per well, 3 wells per condition, 2 independent experiments) (mean  $\pm$  SD; \*\*\*P < .005). (D) Representative fluorescence images from quantifications shown in panel C. Scale bars, 100  $\mu\text{m}$ .



## Discussion

In the present study, we demonstrated that Slc44a2 is involved in the direct adhesion and activation process of neutrophils on VWF. Slc44a2-mediated adhesion and NETosis are HNA 3a/HNA-3b and VWF-A1 domain dependent. These phenomena are potentialized by inflammatory stimulation, low shear rates ( $100 \text{ s}^{-1}$ ), and cell concentration.

Genome-wide association studies have homogeneously identified *SLC44A2* as a new gene associated with VT risk. This was reinforced by mice data we and others obtained showing that absence of Slc44a2 is linked to reduced thrombus formation in the stenosis VT model.<sup>4,5</sup> Until these findings, the pathophysiology of VT was mostly based on the original cascade model of coagulation. Because Slc44a2 does not belong to it, it is of major importance to characterize the biological link between this

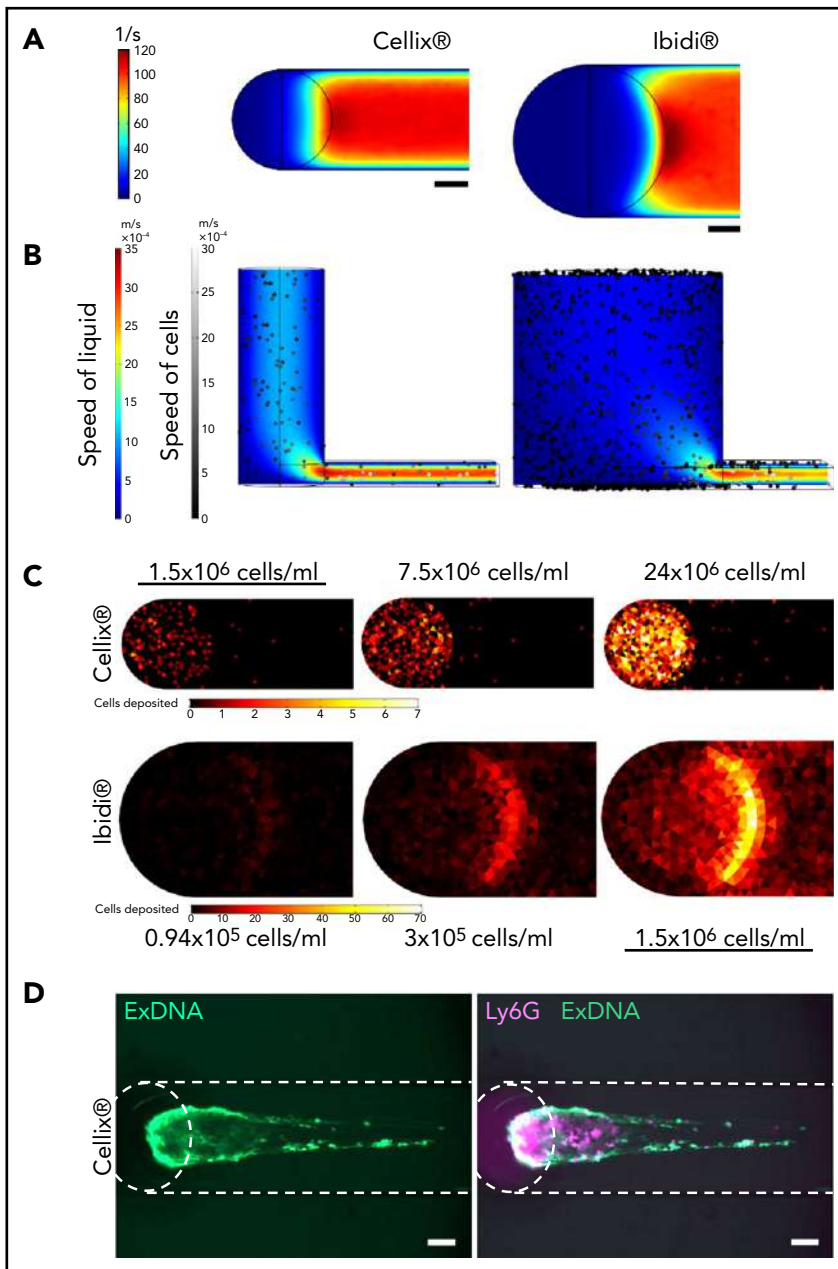


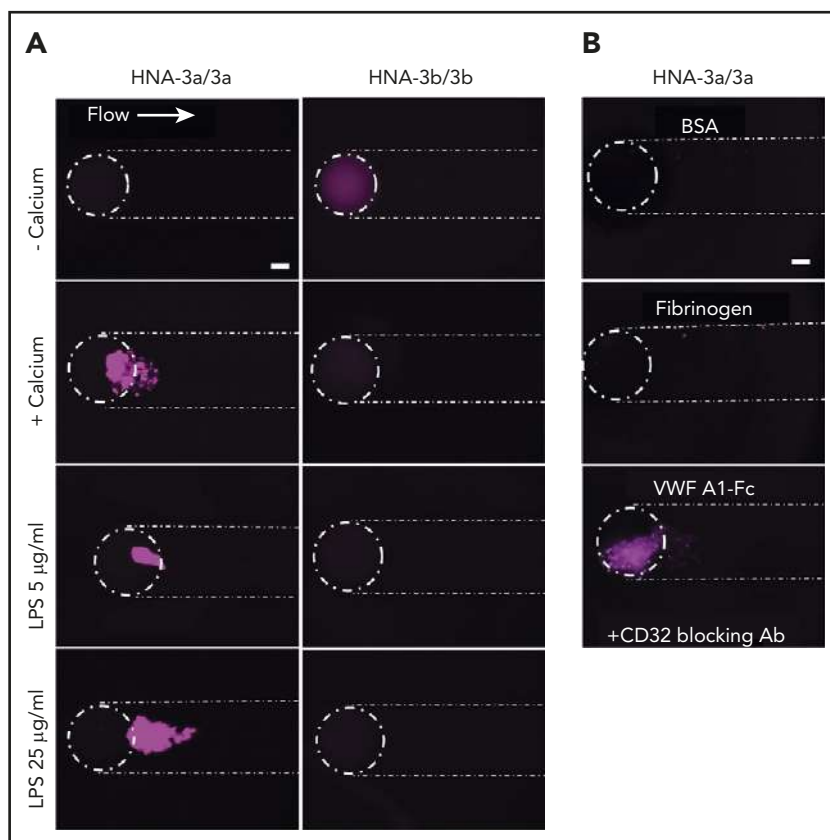
**Figure 5. Numerical simulations of rheological conditions and cell motion in chamber entrance.** (A) Maps of shear rates at chamber bottom wall for Cellix chamber for flow of 4  $\mu\text{L}/\text{min}$  (left panel) and for Ibidi chamber for flow of 10  $\mu\text{L}/\text{min}$  (right panel) corresponding experimentally to a desired shear rate of 100  $\text{s}^{-1}$  in the observation section of the chamber. Scale bars, 200  $\mu\text{m}$ . (B) Map of fluid and cell velocity in a sagittal cut of the Cellix chamber (left panel) or the Ibidi chamber entrance (right panel) along its symmetry axis. Cells are simulated as spheres. (C) Number of deposited cells at  $t = 60$  seconds as a function of the cell concentration perfused into the chambers. (D) Representative images of fluorescently labeled neutrophils (Ly6G, pink) and extracellular DNA (exDNA, green) after perfusion (100  $\text{s}^{-1}$  shear rate) on VWF in a Cellix flow chamber ( $n = 3$ ). Scale bars, 100  $\mu\text{m}$ . Dashed lines have been added to delimit the flow channels and the well entrance.

protein and VT. In the current study, we aimed to understand how the *SLC44A2* gene and the lead rs2288904 variant (461G>A; Arg154Gln; HNA-3a/HNA-3b) could affect *Slc44a2* function in thrombosis through neutrophils. This last decade, neutrophils and VWF have been shown to play a central role in VT.<sup>17,20,25</sup> VWF is known to be an important protein in hemostasis, as it mediates platelet adhesion to the subendothelial matrix and is involved in inflammation processes (for review, see Kawecki et al<sup>26</sup>) that are crucial during VT development. *Slc44a2* has been previously shown as a binding partner for VWF.<sup>10</sup> However, how the Arg154Gln polymorphism could directly modulate cell interaction with VWF at low shear rates had not been studied. Constantinescu-Bercu et al recently reported that *Slc44a2* could permit adhesion of neutrophils to primed platelets adhered at high shear rates (1000  $\text{s}^{-1}$ ) on VWF via their  $\alpha_{\text{IIb}}\beta_3$  receptors.<sup>11</sup> It is indeed possible that neutrophils do not need platelets to bind the VWF-A1 domain, as suggested originally by Bayat et al.<sup>10</sup> A very recent work suggested that

*Slc44a2* could regulate platelet mitochondrial function, thus affecting platelet adenosine 5'-diphosphate production.<sup>5</sup> The fact that VWF and neutrophils are essential in VT does not necessarily mean that platelets are essential to recruit neutrophil at the endothelium even if they participate in the process.

Because HNA-3b expression is associated with a decreased risk for VT in patients,<sup>1,2</sup> we imagined a possible loss of function of *Slc44a2*/HNA-3b leading to a reduced binding of *Slc44a2* to VWF. We used HEK293T transfected cells, neutrophils, and mice to assess *Slc44a2*'s importance in the mechanisms of neutrophil adhesion to VWF in vitro and in vivo. We observed that the HNA-3a/HNA-3b epitope had no effect on neutrophil rolling (200-500  $\mu\text{m}/\text{s}$ ) when perfused on a VWF-coated matrix. However, our data show that *Slc44a2*/HNA-3a, but not *Slc44a2*/HNA-3b, is crucial for HEK293T or neutrophil slow rolling (0-10  $\mu\text{m}/\text{s}$ ) to VWF at venous shear rates (100  $\text{s}^{-1}$ ).

**Figure 6. Neutrophil activation on VWF at  $100\text{ s}^{-1}$  is HNA-3a, calcium, and VWF A1-domain dependent and can be exacerbated by LPS challenge.** (A) Representative images of HNA-3a or HNA-3b neutrophils (anti-Ly6G IgG) submitted to a  $100\text{ s}^{-1}$  shear rate in the absence or presence of calcium or preactivated with LPS prior to perfusion (5 or  $25\text{ }\mu\text{g}/\text{mL}$ ) (Cellix flow chambers,  $n = 3$  donors per genotype). (B) Representative images of HNA-3a neutrophils perfused at a  $100\text{ s}^{-1}$  shear rate on immobilized BSA, fibrinogen, or VWF A1-Fc domain. Neutrophil Fc receptors were blocked with anti-CD32 antibody (Ab) for A1 domain experiments. Scale bars,  $100\text{ }\mu\text{m}$ . Lines delimit flow channels and the well entrance ( $n = 3$  donors per genotype).



When looking at our rolling data, we must consider that 2% of total tracked slow-rolling cells in the HNA-3a group can be relevant. The majority (60% to 75%) of the total tracked cells are non-sedimented (not close enough to the wall).  $\text{MnCl}_2/\text{calcium}$  was used as positive control to determine the maximal percentage of slow-rolling neutrophils.  $\text{MnCl}_2$  forces integrins to stay in their active conformation, maximizing cell adhesion on an integrin substrate such as VWF. A total of  $28\% \pm 8\%$  of the total cells were observed in this positive control group representing the 100% slow rolling/adhesion (supplemental Figure 2). Moreover, our *in vivo* data confirm that Slc44a2 plays a significant role in neutrophil recruitment at the vessel wall in mice.

Despite the fact that HEK293T/HNA-3a cells do not express  $\beta_2$  integrins,<sup>27</sup> they adhere more on VWF than HEK293T/HNA-3b cells. However, subsequent integrin activation could potentialize Slc44a2-mediated adhesion of neutrophils, as integrins have been described as playing a major role in leukocyte adhesion.<sup>28</sup> The utilization of a  $\beta_2$ -blocking antibody on neutrophils was not enough to abolish neutrophil adhesion on VWF. Altogether, these observations confirm that Slc44a2 can induce cell adhesion on VWF under flow independently of integrins. However, we cannot exclude that  $\beta_2$  integrins are not involved further in the process of neutrophil recruitment to VWF. Indeed, our results and previous findings<sup>10</sup> suggest that VWF/Slc44a2 interaction could induce neutrophil and integrin activation, thus consolidating the cell adhesion process. In TRALI, for instance, anti-HNA-3a antibodies have been shown to activate neutrophils.<sup>14</sup> VWF may have a comparable effect. Bayat et al published evidence that following VWF binding to Slc44a2, VWF, Slc44a2, and Mac-1 ( $\alpha_M\beta_2$ ) form a trimolecular complex at the neutrophil

surface.<sup>10</sup> In addition, Constantinescu-Bercu et al pointed out that Slc44a2 engagement with  $\alpha_{IIb}\beta_3$  could induce Slc44a2-mediated signaling that participates in neutrophil integrin activation. These observations can lead us to expect an “inside-out” signaling. We observed that neutrophils purified from EDTA-anticoagulated blood showed even less adhesion on VWF than neutrophils after  $\beta_2$  blockade (data not shown). Chelation of divalent cations may affect a possible Slc44a2-mediated calcium mobilization involved in the adhesion process. An older study also identified the Slc44a2-coding gene as being able to activate the NF- $\kappa$ B pathway.<sup>29</sup> Interestingly, this pathway is essential for tissue factor expression in VT.<sup>30</sup>

We have seen that a second hit can significantly affect Slc44a2-mediated neutrophil slow rolling to VWF under flow. In order to track cells upon LPS activation we used a dye incorporating membranes. This dye may have further contributed to cell activation. The dye effect was dose dependent (data not shown), and it increased the rolling background of HNA-3a and HNA-3b neutrophils.

HNA-3a expression, but also special rheological conditions or additional inflammatory stimuli (such as TNF- $\alpha$  or LPS), can stimulate NETosis. We thus tested different dyes for NETosis observation (such as anti-Ly6g-antibodies and Calcein) to exclude some dye-dependent artifact. The fact that HNA-3b<sup>+</sup> neutrophils are protected from increased adhesion and activation on VWF despite LPS activation supports our 2-hit hypothesis in which cells need 2 priming events to present a proinflammatory profile. These results complete observations from the work of Constantinescu-Bercu et al that showed that neutrophils formed NETs when

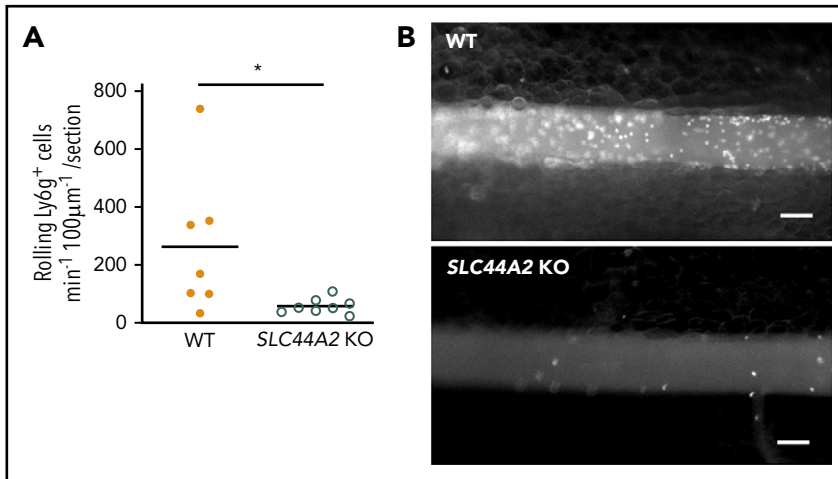


**Figure 7. Slc44a2 is essential for neutrophil recruitment at the vessel wall following endothelial activation.** Intravital microscopy was performed on mesenteric venules of mice deficient in Slc44a2 protein (*SLC44A2* KO mice) after intraperitoneal histamine challenge. (A) Quantification of neutrophil rolling on mesenteric venules in wild-type (WT) and *SLC44A2* KO mice (wild-type, orange circles, n = 7 venules in 3 mice; *SLC44A2* KO, green circles n = 8 venules in 3 mice). (B) Representative images showing reduced neutrophil recruitment in mesenteric venules of *SLC44A2* KO mice after staining of endogenous rolling neutrophils by infusion of an Alexa Fluor 660-anti-Ly6g antibody (bars represent means; \**P* < .05). Scale bars, 100 μm.

adhered to platelets through the  $\alpha_{IIb}\beta_3$  integrin<sup>11</sup> and suggest that Slc44a2 could be a mechanosensor able to modulate cell activation in response to flow. NETosis is an active process following neutrophil activation and is crucial during VT.<sup>18,20</sup> NETs form a matrix for cell (platelets and red blood cells)<sup>31</sup> or microparticle adhesion<sup>32</sup> and represent a thrombogenic surface exposing tissue factor<sup>33</sup> or factor XII.<sup>18</sup>

Our *in vivo* results obtained in the histamine-induced endothelial degranulation model in mice support that Slc44a2 deficiency could delay both neutrophil recruitment and activation on a degranulated endothelium too. This may explain the phenotype of *SLC44A2* KO mice that formed smaller thrombi when submitted to the deep vein thrombosis stenosis model.<sup>4</sup>

VWF and NETs are crucial in VT pathogenesis. They are also involved in other pathologies linked to inflammation such as stroke or myocardial ischemia/reperfusion injury.<sup>34-37</sup> HNA-3a has also been associated with stroke.<sup>2</sup> Stroke involves the VWF-A1 domain,<sup>38</sup> which is the one important in Slc44a2-mediated adhesion as well. Our work suggests that GPIb may not be the only receptor involved when we talk about VWF-A1-associated thromboinflammatory pathogenesis. Slc44a2 has to be taken into consideration. Also, the platelet GPIb receptor and Slc44a2 may bind to the same epitope on the VWF-A1 domain. VWF is released by endothelial cells through a constitutive pathway and Weibel-Palade bodies release. VWF released from the storage compartment is of high molecular weight<sup>39</sup> and is released with a relatively high concentrations of calcium ions<sup>40</sup> upon vascular injury or inflammatory stimulation. Our work suggests that Slc44a2 may be involved not only in VT but also in more pathologies than we originally thought in the inflammation field.

HNA-3b homozygous individuals being rare (6% of White population),<sup>22</sup> it is easy to imagine that previous work focusing on neutrophil adhesion and VWF used HNA-3a-positive donors. Here, we point out the necessity to check on the HNA-3a/3b genotype of blood donors before working with VWF.

This paper presents some limitations. The flow chambers used in this study do not exactly mimic human veins; they are devoid of vein valves (no valve-associated flow disturbances), wall

plasticity, and pulsatile blood flow. Our system does not include other blood cells that can possibly potentialize interactions. However, this model allowed us to determine in a simple calibrated system how Slc44a2 impacts neutrophil cell velocity on a VWF matrix. We could determine the effect of shear rates, cell concentration, and inflammatory prestimulation and observe NETosis in specific rheologic condition. The use of LPS to mimic inflammation reflects not sterile inflammation but infection-related inflammation. We only used young male mice (12 weeks old). VT is not gender exclusive. However, this allowed us to reduce data variability that could have been influenced by female estrous cycles. Despite the fact that the age is important in the study of age-related thrombosis, to have young mice with less abdominal fat allowed us to study the involvement of a protein in a physiological process.

In summary, we propose a new mechanism of neutrophil adhesion and activation that connects inflammation to thrombosis in veins. This mechanism involves the VWF-A1 domain and can induce neutrophil activation and NETosis. Other studies are thus warranted to better understand the mechanisms of Slc44a2/VWF molecular interaction and how this interaction can also influence neutrophil activation. As Slc44a2 is expressed by neutrophils, platelets, and endothelial cells, it would be interesting to determine the relative contribution of Slc44a2 from these cells in thromboinflammatory disorders. Shutting down Slc44a2 function would allow us to target thrombosis specifically, without affecting hemostasis, which would reduce the risk of hemorrhagic complications that are associated with actual prophylactic anticoagulant therapies.

## Acknowledgments

The authors thank Thomas E. Carey (University of Michigan, Ann Arbor, MI) for the floxed *SLC44A2* KO mice; Michel Grino, Matthias Canault, and Cécile Denis for helpful discussions; and Brian Curtis and Daniel Bougie for providing us with the HEK293T transfected cells.

This work was supported by Trombosestichting Nederland (#2015-4) and the French National Research Agency (grant ANR-17-CE14-0003-01 (G.M.T)).

## Authorship

Contribution: G.Z., P.R., B.J.M.v.V., M.-C.A., P.J.L., P.-E.M., and G.M.T. contributed to experimental design; G.Z., J.T., P.R., V.T., C.X.M., P.L.,

B.J.M.v.V., M.-C.A., P.J.L., P.-E.M., and G.M.T. performed experiments and analyzed data; G.Z., P.R., P.-E.M., and G.M.T. wrote the paper; and all authors commented on manuscript drafts and approved the final version.

Conflict-of-interest disclosure: The authors declare no competing financial interests.

ORCID profiles: G.Z., 0000-0002-2017-0248; J.T., 0000-0001-6135-5962; V.T., 0000-0003-0283-3498; P.J.L., 0000-0002-7937-3429; G.M.T., 0000-0003-4502-7154.

Correspondence: Grace M. Thomas, INSERM UMR-S 1263 Center for CardioVascular and Nutrition Research - C2VN, Faculté de Médecine Timone, 3<sup>È</sup>me Étage Aile Bleue, 27 Bd Jean Moulin, 13385 Marseille, France; e-mail: grace.thomas@univ-amu.fr.

## Footnotes

Submitted 22 July 2020; accepted 11 January 2021; prepublished online on *Blood* First Edition 8 February 2021. DOI 10.1182/blood.2020008345.

To access data and protocols, contact the corresponding author (grace.thomas@univ-amu.fr).

The online version of this article contains a data supplement.

There is a *Blood* Commentary on this article in this issue.

The publication costs of this article were defrayed in part by page charge payment. Therefore, and solely to indicate this fact, this article is hereby marked "advertisement" in accordance with 18 USC section 1734.

## REFERENCES

1. Germain M, Chasman DI, de Haan H, et al; Cardiogenics Consortium. Meta-analysis of 65,734 individuals identifies TSPAN15 and SLC44A2 as two susceptibility loci for venous thromboembolism. *Am J Hum Genet*. 2015; 96(4):532-542.
2. Hinds DA, Buil A, Ziemek D, et al; META-STROKE Consortium, INVENT Consortium. Genome-wide association analysis of self-reported events in 6135 individuals and 252 827 controls identifies 8 loci associated with thrombosis. *Hum Mol Genet*. 2016;25(9): 1867-1874.
3. Tilburg J, Adili R, Nair TS, et al. Characterization of hemostasis in mice lacking the novel thrombosis susceptibility gene Slc44a2. *Thromb Res*. 2018;171:155-159.
4. Tilburg J, Coenen DM, Zirka G, et al. SLC44A2 deficient mice have a reduced response in stenosis but not in hypercoagulability driven venous thrombosis. *J Thromb Haemost*. 2020; 18(7):1714-1727.
5. Bennett JA, Mastrangelo MA, Ture SK, et al. The choline transporter Slc44a2 controls platelet activation and thrombosis by regulating mitochondrial function. *Nat Commun*. 2020;11(1):3479.
6. Greinacher A, Wesche J, Hammer E, et al. Characterization of the human neutrophil alloantigen-3a. *Nat Med*. 2010;16(1):45-48.
7. Curtis BR, Sullivan MJ, Holyst MT, Szabo A, Bougie DW, Aster RH. HNA-3a-specific antibodies recognize choline transporter-like protein-2 peptides containing arginine, but not glutamine at Position 154. *Transfusion*. 2011;51(10):2168-2174.
8. Kanack AJ, Peterson JA, Sullivan MJ, Bougie DW, Curtis BR, Aster RH. Full-length recombinant choline transporter-like protein 2 containing arginine 154 reconstitutes the epitope recognized by HNA-3a antibodies. *Transfusion*. 2012;52(5):1112-1116.
9. Flesch BK, Wesche J, Berthold T, et al. Expression of the CTL2 transcript variants in human peripheral blood cells and human tissues. *Transfusion*. 2013;53(12):3217-3223.
10. Bayat B, Tjahjono Y, Berghöfer H, et al. Choline transporter-like protein-2: new von Willebrand factor-binding partner involved in antibody-mediated neutrophil activation and transfusion-related acute lung injury. *Arterioscler Thromb Vasc Biol*. 2015;35(7): 1616-1622.
11. Constantinescu-Bercu A, Grassi L, Frontini M, Salles-Crawley II, Woollard K, Crawley JT. Activated  $\alpha_{IIb}\beta_3$  on platelets mediates flow-dependent NETosis via SLC44A2. *eLife*. 2020; 9:e53353.
12. Mair DC, Eastlund T. The pathophysiology and prevention of transfusion-related acute lung injury (TRALI): a review. *Immunohematology*. 2010;26(4):161-173.
13. Berthold T, Muschter S, Schubert N, et al. Impact of priming on the response of neutrophils to human neutrophil alloantigen-3a antibodies. *Transfusion*. 2015;55(6 Pt 2): 1512-1521.
14. Thomas GM, Carbo C, Curtis BR, et al. Extracellular DNA traps are associated with the pathogenesis of TRALI in humans and mice. *Blood*. 2012;119(26):6335-6343.
15. Caudrillier A, Kessenbrock K, Gilliss BM, et al. Platelets induce neutrophil extracellular traps in transfusion-related acute lung injury. *J Clin Invest*. 2012;122(7):2661-2671.
16. Darbousset R, Thomas GM, Mezouar S, et al. Tissue factor-positive neutrophils bind to injured endothelial wall and initiate thrombus formation. *Blood*. 2012;120(10):2133-2143.
17. Brill A, Fuchs TA, Savchenko AS, et al. Neutrophil extracellular traps promote deep vein thrombosis in mice. *J Thromb Haemost*. 2012;10(1):136-144.
18. von Brühl M-L, Stark K, Steinhart A, et al. Monocytes, neutrophils, and platelets cooperate to initiate and propagate venous thrombosis in mice in vivo. *J Exp Med*. 2012; 209(4):819-835.
19. Fuchs TA, Brill A, Wagner DD. Neutrophil extracellular trap (NET) impact on deep vein thrombosis. *Arterioscler Thromb Vasc Biol*. 2012;32(8):1777-1783.
20. Martinod K, Demers M, Fuchs TA, et al. Neutrophil histone modification by peptidylarginine deiminase 4 is critical for deep vein thrombosis in mice. *Proc Natl Acad Sci USA*. 2013;110(21):8674-8679.
21. Bougie DW, Peterson JA, Kanack AJ, Curtis BR, Aster RH. Transfusion-related acute lung injury-associated HNA-3a antibodies recognize complex determinants on choline transporter-like protein 2. *Transfusion*. 2014; 54(12):3208-3215.
22. Bowens KL, Sullivan MJ, Curtis BR. Determination of neutrophil antigen HNA-3a and HNA-3b genotype frequencies in six racial groups by high-throughput 5' exonuclease assay. *Transfusion*. 2012;52(11):2368-2374.
23. Wang P, Wu P, Anthes JC, Siegel MI, Egan RW, Billah MM. Interleukin-10 inhibits interleukin-8 production in human neutrophils. *Blood*. 1994;83(9):2678-2683.
24. Fuchs TA, Abed U, Goosmann C, et al. Novel cell death program leads to neutrophil extracellular traps. *J Cell Biol*. 2007;176(2): 231-241.
25. Brill A, Fuchs TA, Chauhan AK, et al. von Willebrand factor-mediated platelet adhesion is critical for deep vein thrombosis in mouse models. *Blood*. 2011;117(4):1400-1407.
26. Kawecki C, Lenting PJ, Denis CV. von Willebrand factor and inflammation. *J Thromb Haemost*. 2017;15(7):1285-1294.
27. Gupta V, Alonso JL, Sugimori T, Essafi M, Xiong JP, Arnaout MA. Role of the  $\beta$ -subunit arginine/lysine finger in integrin heterodimer formation and function. *J Immunol*. 2008; 180(3):1713-1718.
28. Kuijpers TW, Van Lier RA, Hamann D, et al. Leukocyte adhesion deficiency type 1 (LAD-1)/variant. A novel immunodeficiency syndrome characterized by dysfunctional beta2 integrins. *J Clin Invest*. 1997;100(7): 1725-1733.
29. Matsuda A, Suzuki Y, Honda G, et al. Large-scale identification and characterization of human genes that activate NF-kappaB and MAPK signaling pathways. *Oncogene*. 2003; 22(21):3307-3318.
30. Li Y-D, Ye B-Q, Zheng S-X, et al. NF-kappaB transcription factor p50 critically regulates tissue factor in deep vein thrombosis. *J Biol Chem*. 2009;284(7):4473-4483.
31. Fuchs TA, Brill A, Duerschmied D, et al. Extracellular DNA traps promote thrombosis. *Proc Natl Acad Sci USA*. 2010;107(36): 15880-15885.
32. Thomas GM, Brill A, Mezouar S, et al. Tissue factor expressed by circulating cancer cell-derived microparticles drastically increases the incidence of deep vein thrombosis in mice. *J Thromb Haemost*. 2015;13(7): 1310-1319.
33. Kambas K, Chrysanthopoulou A, Vassilopoulos D, et al. Tissue factor expression

- in neutrophil extracellular traps and neutrophil derived microparticles in antineutrophil cytoplasmic antibody associated vasculitis may promote thromboinflammation and the thrombophilic state associated with the disease. *Ann Rheum Dis*. 2014;73(10):1854-1863.
34. Zhao B-Q, Chauhan AK, Canault M, et al. von Willebrand factor-cleaving protease ADAMTS13 reduces ischemic brain injury in experimental stroke. *Blood*. 2009;114(15):3329-3334.
35. Hillgruber C, Steingraber AK, Pöppelmann B, et al. Blocking von Willebrand factor for treatment of cutaneous inflammation. *J Invest Dermatol*. 2014;134(1):77-86.
36. Savchenko AS, Borissoff JI, Martinod K, et al. VWF-mediated leukocyte recruitment with chromatin decondensation by PAD4 increases myocardial ischemia/reperfusion injury in mice. *Blood*. 2014;123(1):141-148.
37. Dhanesha N, Prakash P, Doddapattar P, et al. Endothelial cell-derived von Willebrand factor is the major determinant that mediates von willebrand factor-dependent acute ischemic stroke by promoting postischemic thromboinflammation. *Arterioscler Thromb Vasc Biol*. 2016;36(9):1829-1837.
38. Denorme F, Martinod K, Vandenbulcke A, et al. The von Willebrand Factor A1 domain mediates thromboinflammation, aggravating ischemic stroke outcome in mice [published online ahead of print 27 February 2020]. *Haematologica*. doi:10.3324/haematol.2019.241042.
39. Wagner DD. Cell biology of von Willebrand factor. *Annu Rev Cell Biol*. 1990;6(1):217-246.
40. Poisner A, Trifaro J-M. Common properties in the mechanisms of synthesis, processing and storage of secretory products. In: *The Secretory Granule*. Elsevier/North Holland; 1982: 387-407.